NANO LETTERS
Cite This: Nano Lett. 2019, 19, 2032−2036
Letter
pubs.acs.org/NanoLett

Living Supramolecular Polymerization of Rod−Coil Block Copolymers: Kinetics, Origin of Uniformity, and Its Implication

Liang Gao, Jiaping Lin,* Liangshun Zhang, and Liquan Wang*

Shanghai Key Laboratory of Advanced Polymeric Materials, Key Laboratory for Ultrafine Materials of Ministry of Education, State Key Laboratory of Bioreactor Engineering, School of Materials Science and Engineering, East China University of Science and Technology, Shanghai 200237, China

Supporting Information

ABSTRACT: We conduct Brownian dynamics simulations to explore the kinetics of living supramolecular polymerization using seeded growth of rod−coil block copolymers as a model system. We model the kinetics of supramolecular polymerization by developing kinetic theory for classical living covalent polymerization with length-dependent rate coefficients. The rate coefficient in the proposed kinetics theory decreases with increasing cylindrical micelle length, which is attributed to micelle rigidity and unique diffusion behavior. Like living covalent polymerization, living supramolecular polymerization can produce low-dispersity assemblies with rigidity via different mechanisms. The results nicely explain the available experimental observations.

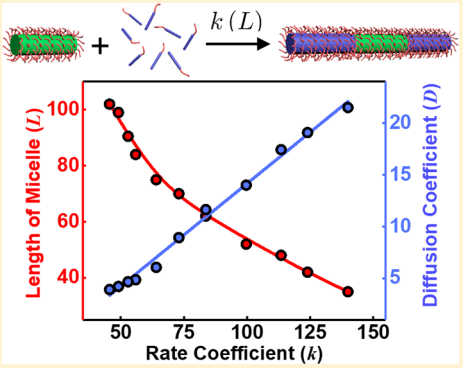

KEYWORDS: *Living supramolecular polymerization, rod−coil copolymer, kinetics, Brownian dynamics*

Living supramolecular polymerization (LSP) has emerged as a versatile and efficient route to create assemblies with controlled dimensions and diverse nanoarchitectures.[1−5] For example, living crystallization-driven self-assembly (CDSA) based on diblock copolymers in which one of the blocks is crystalline has been used to create cylindrical micelles, block comicelles, and other complex nanoarchitectures in a controlled fashion.[6−10] Unlike the well-established living covalent polymerization of monomers, LSP is a newer research field that has only recently attracted attention.[11−17] LSP enables the formation of assemblies with low dispersity, similar to living covalent polymerization.[18−20] The origin of the low dispersity, one of the salient features of LSP, remains a mystery. To determine the origin of the low dispersity, the kinetics of LSP must be sufficiently explored; however, the exploration remains challenging.

Very recently, Manners et al. probed the kinetics of LSP using seeded growth of PFS-*b*-PDMS block copolymers, where PFS and PDMS are poly(ferrocenyldimethylsilane) and polydimethylsiloxane, respectively, as a model of living CDSA systems.[21] Their data fitting with constant rate coefficients revealed that LSP kinetics do not exhibit a first-order dependence of the growth rate on the unimer concentration as anticipated based on living covalent polymerization.[21,22] This data fitting is undoubtedly mathematically correct, but the obtained results cannot physically explain the deviation from first-order kinetics. They postulated that the difference may be the result of the combined influence of the chain conformation and chain polydispersity on the addition of the unimer to micelle termini.[21] Moreover, in numerous LSP experimental attempts to create cylindrical micelles, the lengths of cylindrical micelles were also found to deviate from the theoretical values predicted based on living covalent polymerization.[23,24] In this Communication, we conducted Brownian dynamics (BD) simulations of seeded growth of rod−coil block copolymers to account for the deviation from first-order behavior and to obtain insight into the origin of low-dispersity assemblies via theoretically analyzing LSP kinetics.

We first considered the self-assembly of rod−coil block copolymers in selective solvents and prepared preassembled seeds. A coarse-grained model of $\mathbf{R}_m\mathbf{C}_n$ was constructed for the rod−coil block copolymer (Figure S1), where **R**, **C**, and the subscripts denote the rod block, coil block, and bead number of each block, respectively. According to the aggregate morphologies for different copolymer molecular structures (Figure S2), $\mathbf{R}_6\mathbf{C}_3$ was chosen to obtain cylindrical micelles. Furthermore, a morphological diagram of the initial copolymer concentration C_0 versus the interaction strength ε_{RR} was constructed (Figure S3). The region between the spinodal and binodal lines is a metastable region where nucleation growth can occur. Self-nucleation is impossible in the metastable region, and self-assembly can occur only by adding nucleators. In addition, we learned that a cylindrical micelle can act as a nucleator due to its incompletely covered ends.[25−27] Note that the preassembled cylindrical micelles can retain their shapes

Received: January 14, 2019
Revised: February 8, 2019
Published: February 11, 2019

DOI: 10.1021/acs.nanolett.9b00163
Nano Lett. 2019, 19, 2032−2036

and structures in the metastable region (Figure S5). Therefore, cylindrical micelles can serve as seeds for further growth through supramolecular polymerization with copolymers in this metastable region.

To prove this supposition, the cylindrical micelles assembled from $\mathbf{R}_6\mathbf{C}_3$ copolymers were subjected to new simulation conditions with added $\mathbf{R}_6\mathbf{C}_3$ copolymers. The concentration C_0^{second} of added unimer varied from 2.0×10^{-4} σ^{-3} to 5.0×10^{-4} σ^{-3} at a fixed interaction strength of 2.5 ε, which is located in the metastable region (Figure S3; σ and ε are the units of length and energy, respectively; the other simulation conditions are given in Section 1 of the SI). The growth of preassembled cylindrical micelles was observed after adding more unimers (Figure 1a). As shown in the snapshots of the

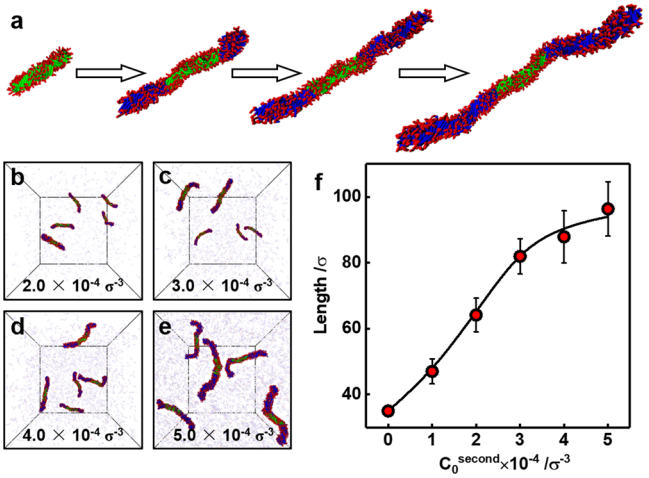

Figure 1. (a) Living growth of preassembled cylindrical micelles. (b–e) Morphologies of the cylindrical micelles after adding copolymers with various concentrations C_0^{second}. (f) Dependence of the number-average contour length of elongated cylindrical micelles on C_0^{second}. All the micelles were obtained at a simulation time of 1.0×10^5 τ.

simulations (Figure 1b–e), the added copolymers do not form new micelles and the longer elongated micelles were obtained at higher concentrations C_0^{second}. The elongated parts present at the ends of the cylindrical micelles with equal length, suggesting that the growth starts from two "living" ends simultaneously (Figure S6). Figure 1f displays the number-average contour length of the elongated micelles as a function of the concentration C_0^{second} of added copolymers at a fixed simulation time. With increasing C_0^{second}, longer cylindrical micelles are obtained. The small error bars in Figure 1f indicate the narrow length distribution of the elongated micelles. This growth is a living supramolecular polymerization (LSP) process.

We examined the structural characteristics of the cylindrical seeds and elongated micelles to gain insight into the mechanism of this growth process. As shown in Figure 2a, the rod blocks within the cylindrical core are interdigitatedly packed. The orientation angle is defined as the angle between the direction vector of the rod block and the chosen direction vector (see the sketch in Figure 2a). The periodic variation in the orientation angle indicates that the rod blocks are orderly packed in a cholesteric LC manner (Figure 2b).[28] The origin of the helical order in the micelle core is the entropy associated with the excluded volume of the coil blocks, and the chirality is randomly determined (Figure S4).[29,30] The coil blocks make

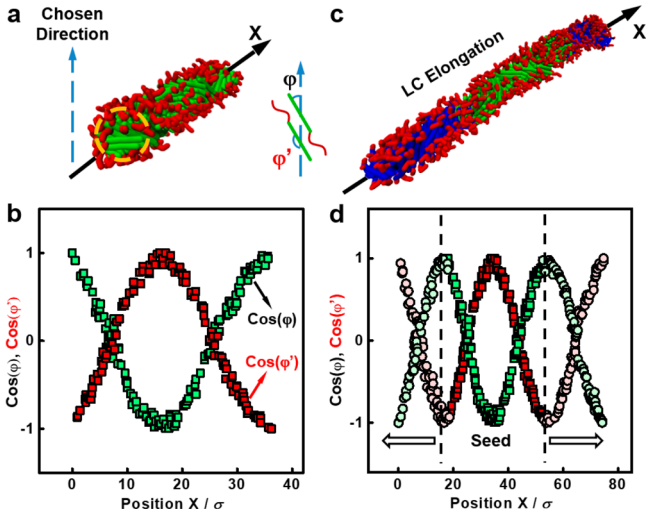

Figure 2. (a) 3D view of the typical structure of the cylindrical seed and definitions of the orientation angles. (b) Variations in the cosine of the orientation angles along the long axis X of the cylindrical micelles. (c) 3D view of the typical structure of the elongated micelle, where the seed and elongated parts are marked as green and blue, respectively. (d) Variations in the cosine of the orientation angles along the long axis X of the cylindrical micelles.

up the coronas that surround the LC cylindrical cores with the two incompletely covered ends (see the marked region in Figure 2a). The exposed ends serve as "living" ends to induce further self-assembly. Figure 2c and d shows the typical elongated micelles and variations in the orientation angles, respectively. The added copolymers join the seed ends and twist to align in a cholesteric LC manner, resulting in a twisting structure with elongated parts. Unlike the CDSA, which occurs via chain folding in a micelle core,[6−8] this living assembly is driven by the epitaxial growth of a cholesteric LC-like structure, which we name liquid-crystallization-driven self-assembly (LCDSA).

This living assembly, i.e., LSP, resembles classical living covalent polymerization of monomers but occurs on a supramolecular scale. The preassembled seeds and added copolymers can be considered as active polymer chains and monomers, respectively. To judge whether this supramolecular polymerization satisfies the principle of living covalent polymerization, the growth kinetics were further examined. We investigated the growth kinetics of cylindrical seeds with various lengths, where C_0^{second} and ε_{RR} were fixed at 3.0×10^{-4} σ^{-3} and 2.6 ε, respectively. Figure 3a and b displays the simulation morphologies of the initial cylindrical seeds (62 σ) and the elongated cylindrical micelles at a growth time of 1.0×10^5 τ; the morphologies of the longer seed (120 σ) are shown in Figure 3c and d. It can be seen from the simulated morphologies that the short cylindrical seed can consume more unimers in the same growth time.

The length of the elongated cylindrical micelle L is directly related to the consumption of added copolymers:

$$L = L_{seed} + AN \quad (1)$$

where L_{seed} is the length of the seed; A represents the contribution of a copolymer to the length of the cylindrical micelle; and N is the amount of added copolymers consumed per seed. The variation in consumed unimers N with the growth time for cylindrical seeds with various lengths is shown

DOI: 10.1021/acs.nanolett.9b00163
Nano Lett. 2019, 19, 2032−2036

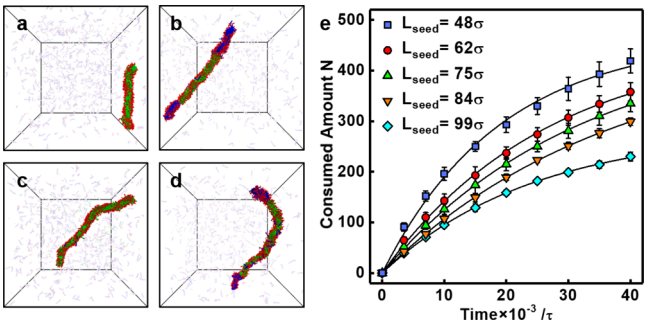

Figure 3. (a–d) Morphologies of cylindrical seeds with different lengths and elongated cylindrical micelles: (a, b) L_{seed} = 62 σ and (c, d) L_{seed} = 120 σ. (e) Variations in the amount of N consumed by added copolymers as a function of simulation time for cylindrical seeds with various lengths L_{seed}.

in Figure 3e. The added copolymers are quickly consumed initially and then consumption slows over time. The shorter cylindrical micelle consumes unimers more quickly, and the growth rate is influenced by the length of the cylinder. These results suggest that the rate coefficient of propagation depends on the length of the cylinder.

According to the first-order kinetics of living covalent polymerizations of monomers,[22] the living growth of cylindrical micelles via unimer incorporation is described as $dN/dt = k(C_0^{second} - NC_0^{seed})$, where C_0^{second} and C_0^{seed} are the initial concentrations of the added copolymers and the micelle seeds, respectively, and t is the growth time (for details, see Section 6 of the SI). From this equation, we can directly calculate the rate coefficient k as $k = \Delta N/[(C_0^{second} - NC_0^{seed})\Delta t]$ for the discrete kinetics data shown in Figure 3e.[31,32] Figure 4a shows the variation in k as a function of the micelle length L. The k value decreases as the L value increases, implying that the LSP kinetics deviates from first-order kinetics (constant k). Such deviation can also be seen

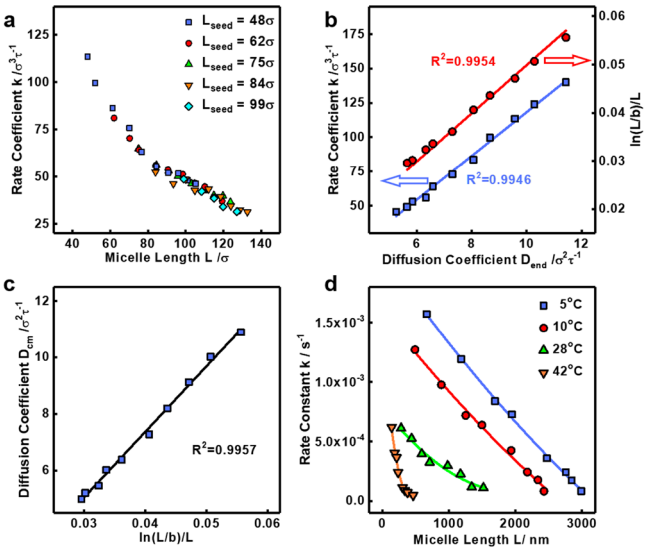

Figure 4. (a) Variations in the rate coefficient k with micelle length L. (b) Linear dependences of k on diffusion coefficient D_{end}, and D_{end} on $\ln(L/b)/L$. (c) Linear dependence of the diffusion coefficient D_{cm} on $\ln(L/b)/L$. (d) Variation in the rate coefficient k with micelle length. The rate coefficients were obtained via analyzing the kinetics data in ref 21 with eq 2.

from the plot of $\ln(N_{final} - N(t))$ versus time t (for details, see Figure S7a). Because the values of k for various L_{seed} fall on the same curve, the dependence of k on L is a universal behavior.

The dependence of k on L can be rationalized by examining the diffusion coefficient D_{end} of living cylindrical ends (the calculation method for the diffusion coefficient is given in Section 1.3 of the SI). As shown in Figure 4b, D_{end} is nearly proportional to $\ln(L/b)/L$, where b is the cross sectional diameter (5 σ) of cylinders. Furthermore, Figure 4b shows a linear dependence of k on D_{end}, indicating that living growth via unimer incorporation is a diffusion-controlled reaction (note that, in the classical kinetics theory of diffusion-controlled reactions, the reaction rate constant is proportional to the diffusion coefficient).[33,34] According to the chemical kinetics theory, the collision frequency between unimers and each seed end is proportional to the product of unimer density and diffusion volume of the end per unit time.[33] The decrease in the diffusion coefficient leads to a decrease in the collision frequency between the ends and the unimers, thereby slowing the growth rate. Such a phenomenon has been reported in numbers of works on polymerization kinetics.[35−37]

The dependence of the diffusion behavior on micelle length can be explained in terms of the rigidity of cylindrical micelles. For a rigid rod, the diffusion coefficient D_{cm} for the center-of-mass is proportional to $\ln(L/b)/L$.[38] We then examined the dependence of D_{cm} on $\ln(L/b)/L$ to understand the rigidity of the cylindrical micelles, and the dependence is presented in Figure 4c. As shown, the diffusion coefficient D_{cm} linearly depends on $\ln(L/b)/L$, which indicates that the cylindrical micelles are inherently rigid. According to the structural characterization and growth mechanism (Figure 2), we concluded that the rigidity of cylindrical micelles is attributed to the ordered packing of rod blocks in the micellar core. In available experiments on the seeded growth of cylindrical or fiber-like micelles,[6−8,19,20] the observed micelles have also been reported to be rigid, consistent with our simulation findings. Note that both the D_{cm} and D_{end} are proportional to $\ln(L/b)/L$ due to negligible contribution of rotational diffusion (for details, see Section 6.4 of the SI). Based on our discovered relationship between k and L (Figure S7b), we proposed a new kinetics equation for the LSP of rod−coil block copolymers:

$$\frac{dN}{dt} = k_c \frac{\ln(L/b)}{L}(C_0^{second} - NC_0^{seed}) \quad (2)$$

where k is represented as $k = k_c \ln(L/b)/L$ with a constant k_c (for details, see Section 6 of the SI). This equation physically explains that the deviation from first-order kinetics is due to the length-dependent coefficient $\ln(L/b)/L$ from limited diffusion.

Very recently, Manners et al. found that the seeded growth of PFS-*b*-PDMS does not follow a first-order dependence of growth rate on unimer concentration when they assumed a constant rate coefficient.[21] Our theory is able to explain this deviation from first-order behavior. Because the cylindrical micelles in living growth are rigid, first-order kinetics with a length-independent rate coefficient cannot be applied to seeded growth of PFS-*b*-PDMS, and the rate coefficient should depend on the length of the assemblies. Therefore, we calculated the rate coefficients by analyzing their experimental results (for details, see Section 6 of the SI). Figure 4d shows the dependence of the rate coefficient on the length of the micelle obtained from the experiments carried out by Manners et al. As shown in Figure 4d, for various temperatures, the rate

DOI: 10.1021/acs.nanolett.9b00163
Nano Lett. 2019, 19, 2032−2036

coefficient k dramatically decreases with increasing micelle length, which is in good agreement with the simulation results shown in Figure 4a.

We should emphasize here that, although the packing manner of rod blocks into LC-like cores in our simulation is different from the crystallization of PFS in the experiments, the LSP exhibits similar growth behaviors. This is due to the fact that they both form cylindrical micelles with rigidity. The diffusion behaviors of rigid cylinders are identical in essence. The kinetic mechanism observed from the simulations can be applicable to PFS−PDMS systems. As the present work is focused on the LSP kinetics, the rod−coil block copolymer could be a suitable model for PFS-*b*-PDMS. Our simulations also indicated that higher concentrations of C_0^{second} or a stronger interaction strength ε_{RR} can promote the living growth of cylindrical micelles (Figures S10 and S11). These findings are also consistent with the available experimental findings that elevated temperatures and higher amounts of poor solvents for crystalline or conjugated segments substantially favor micelle growth.[24]

As longer cylinders grow more slowly than shorter cylinders, uniform length distributions can ultimately be achieved if sufficient unimers for LSP are present. We therefore examined the length distributions of cylinders via the stepwise addition of unimers (note that the stepwise method can control the unimer concentration in the metastable region to avoid self-nucleation growth, which can create new seeds and is unfavorable for low dispersity). The results are shown in Figure 5a (for simulation details, see Section 1.2 of the SI). As

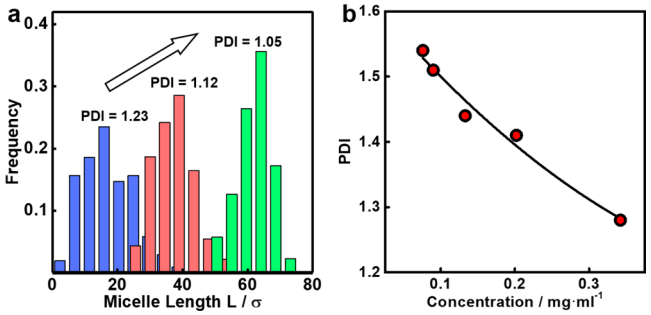

Figure 5. (a) Histograms of the micelle length distribution for micelles obtained through stepwise addition of unimers. The preassembled micelles were formed at $C_0 = 3.0 \times 10^{-4}\ \sigma^{-3}$ and $\varepsilon_{RR} = 2.7\ \varepsilon$ (blue bars), and the concentration of added copolymers in the stepwise process was $2.0 \times 10^{-4}\ \sigma^{-3}$. (b) Variation of PDI with the addition of more unimers, adapted from ref 7.

copolymers are stepwise added, the length distribution becomes narrower, and the PDI decreases from 1.23 to 1.12 and finally to 1.05. This phenomenon agrees well with the experimental findings by Winnik et al. that the length distribution becomes narrower as more copolymers are stepwise added (see Figure 5b adapted from ref 7). These results suggest that low-dispersity assemblies can be realized via LSP of rigid assemblies and that these assemblies originate from the slower growth of longer cylinders with rigidity.

Finally, we compared the LSP of rigid cylinders with the living covalent polymerization of monomers. Chain terminations are absent to maintain living conditions, and products (polymers or assemblies) with a very low polydispersity index (PDI) can be achieved in both polymerizations. Despite the similarities, these methods achieve low dispersity in distinctly different manners. In the living covalent polymerization of monomers, the produced polymers tend to have a low PDI due to the rate of initiation being much faster than the (constant) rate of propagation.[22] By contrast, in the LSP of rigid cylinders, the slower growth of longer cylinders leads to a low PDI of the formed assemblies (note that the initiation, i.e., self-nucleation, is usually very slow, resulting in a broader distribution of the seeds). The first-order kinetics can also apply to the LSP of rigid cylinders, but the rate coefficients must be length dependent. The difference in the uniform mechanisms gives another implication that preparing low-dispersity seeds is not necessary but helpful for accessing low-dispersity micelles via LSP.

In summary, we investigated the kinetics of living supramolecular polymerization of rigid cylinders using seeded growth of rod−coil block copolymers as a model system. The proposed kinetic theory with length-dependent rate coefficients can nicely describe the kinetics of LSP. The growth is a diffusion-controlled process related to the motion of rigid cylinders. The results from the theory are in agreement with available experimental findings. The discovered LSP kinetics could be applied to a wide range of systems bearing similar characteristics: (1) the formed cylindrical micelles are rigid and (2) the attraction between the living ends and the copolymers are strong. The LSP of rod−coil block copolymers can be a promising strategy to construct uniform assemblies, which is of both practical and functional importance.

■ ASSOCIATED CONTENT

Supporting Information

The Supporting Information is available free of charge on the ACS Publications website at DOI: 10.1021/acs.nanolett.9b00163.

Details regarding the model and method, first-step self-assembly of rod−coil block copolymers, kinetics theory for living supramolecular polymerization, origin of the helical order, stability of the cylindrical seeds in the metastable region, diffusion behavior of rigid cylindrical micelles, and effects of concentration of added unimers and interaction strength (PDF)

■ AUTHOR INFORMATION

Corresponding Authors

*E-mail: jlin@ecust.edu.cn (J.L.).
*E-mail: lq_wang@ecust.edu.cn (L.W.).

ORCID

Jiaping Lin: 0000-0001-9633-4483
Liangshun Zhang: 0000-0002-0182-7486
Liquan Wang: 0000-0002-5141-8584

Notes

The authors declare no competing financial interest.

■ ACKNOWLEDGMENTS

This work was supported by the National Natural Science Foundation of China (21774032, 51833003, 51621002, and 21474029). Support from the Project of Shanghai Municipality (16520721900) and the Fundamental Research Funds for the Central Universities (222201714042) is also appreciated.

■ REFERENCES

(1) Mattia, E.; Otto, S. *Nat. Nanotechnol.* **2015**, *10*, 111−119.

DOI: 10.1021/acs.nanolett.9b00163
Nano Lett. 2019, 19, 2032−2036

(2) Mukhopadhyay, R. D.; Ajayaghosh, A. *Science* **2015**, *349*, 241−242.
(3) Ogi, S.; Sugiyasu, K.; Manna, S.; Samitsu, S.; Takeuchi, M. *Nat. Chem.* **2014**, *6*, 188−195.
(4) Mayer, M.; Scarabelli, L.; March, K.; Altantzis, T.; Tebbe, M.; Kociak, M.; Bals, S.; García de Abajo, F. J.; Fery, A.; Liz-Marzán, L. M. *Nano Lett.* **2015**, *15*, 5427−5437.
(5) Zhang, K.; Yeung, M. C.; Leung, S. Y.; Yam, V. W. *Proc. Natl. Acad. Sci. U. S. A.* **2017**, *114*, 11844−11849.
(6) He, W. N.; Xu, J. T. *Prog. Polym. Sci.* **2012**, *37*, 1350−1400.
(7) Wang, X.; Guerin, G.; Wang, H.; Wang, Y.; Manners, I.; Winnik, M. A. *Science* **2007**, *317*, 644−647.
(8) Inam, M.; Cambridge, G.; Pitto-Barry, A.; Laker, Z. P. L.; Wilson, N. R.; Mathers, R. T.; Dove, A. P.; O'Reilly, R. K. *Chem. Sci.* **2017**, *8*, 4223−4230.
(9) Kim, Y. J.; Cho, C. H.; Paek, K.; Jo, M.; Park, M. K.; Lee, N. E.; Kim, Y. J.; Kim, B. J.; Lee, E. *J. Am. Chem. Soc.* **2014**, *136*, 2767−2774.
(10) Qiu, H.; Hudson, Z. M.; Winnik, M. A.; Manners, I. *Science* **2015**, *347*, 1329−1332.
(11) Petzetakis, N.; Dove, A. P.; O'Reilly, R. K. *Chem. Sci.* **2011**, *2*, 955−960.
(12) Ogi, S.; Stepanenko, V.; Sugiyasu, K.; Takeuchi, M.; Wurthner, F. *J. Am. Chem. Soc.* **2015**, *137*, 3300−3307.
(13) Schmelz, J.; Schedl, A. E.; Steinlein, C.; Manners, I.; Schmalz, H. *J. Am. Chem. Soc.* **2012**, *134*, 14217−14225.
(14) Sun, L.; Petzetakis, N.; Pitto-Barry, A.; Schiller, T. L.; Kirby, N.; Keddie, D. J.; Boyd, B. J.; O'Reilly, R. K.; Dove, A. P. *Macromolecules* **2013**, *46*, 9074−9082.
(15) Robinson, M. E.; Nazemi, A.; Lunn, D. J.; Hayward, D. W.; Boott, C. E.; Hsiao, M. S.; Harniman, R. L.; Davis, S. A.; Whittell, G. R.; Richardson, R. M.; De Cola, L.; Manners, I. *ACS Nano* **2017**, *11*, 9162−9175.
(16) Cui, H.; Chen, X.; Wang, Y.; Wei, D.; Qiu, F.; Peng, J. *Soft Matter* **2018**, *14*, 5906−5912.
(17) Beun, L. H.; Albertazzi, L.; van der Zwaag, D.; de Vries, R.; Cohen Stuart, M. A. *ACS Nano* **2016**, *10*, 4973−4980.
(18) Gilroy, J. B.; Gädt, T.; Whittell, G. R.; Chabanne, L.; Mitchels, J. M.; Richardson, R. M.; Winnik, M. A.; Manners, I. *Nat. Chem.* **2010**, *2*, 566−570.
(19) Tao, D.; Feng, C.; Cui, Y.; Yang, X.; Manners, I.; Winnik, M. A.; Huang, X. *J. Am. Chem. Soc.* **2017**, *139*, 7136−7139.
(20) Qian, J.; Li, X.; Lunn, D. J.; Gwyther, J.; Hudson, Z. M.; Kynaston, E.; Rupar, P. A.; Winnik, M. A.; Manners, I. *J. Am. Chem. Soc.* **2014**, *136*, 4121−4124.
(21) Boott, C. E.; Leitao, E. M.; Hayward, D. W.; Laine, R. F.; Mahou, P.; Guerin, G.; Winnik, M. A.; Richardson, R. M.; Kaminski, C. F.; Whittell, G. R.; Manners, I. *ACS Nano* **2018**, *12*, 8920−8933.
(22) Odian, G. *Principles of Polymerization* **2004**, DOI: 10.1002/047147875X.
(23) Gwyther, J.; Gilroy, J. B.; Rupar, P. A.; Lunn, D. J.; Kynaston, E.; Patra, S. K.; Whittell, G. R.; Winnik, M. A.; Manners, I. *Chem. - Eur. J.* **2013**, *19*, 9186−9197.
(24) Tritschler, U.; Gwyther, J.; Harniman, R. L.; Whittell, G. R.; Winnik, M. A.; Manners, I. *Macromolecules* **2018**, *51*, 5101−5113.
(25) Ding, W.; Lin, S.; Lin, J.; Zhang, L. *J. Phys. Chem. B* **2008**, *112*, 776−783.
(26) Lin, S.; Numasawa, N.; Nose, T.; Lin, J. *Macromolecules* **2007**, *40*, 1684−1692.
(27) Liu, X.; Gao, L.; Wang, L.; Zhang, C.; Lin, J. *Acta Polym. Sin.* **2018**, *10*, 1279−1286.
(28) Ciferri, A. *Liq. Cryst.* **1999**, *26*, 489−494.
(29) Horsch, M. A.; Zhang, Z.; Glotzer, S. C. *Phys. Rev. Lett.* **2005**, *95*, 056105.
(30) Horsch, M. A.; Zhang, Z.; Glotzer, S. C. *J. Chem. Phys.* **2006**, *125*, 184903.
(31) McCoy, B. J.; Madras, G. *Chem. Eng. Sci.* **2001**, *56*, 2831−2836.
(32) Butté, A.; Storti, G.; Morbidelli, M. *Macromol. Theory Simul.* **2002**, *11*, 37−52.
(33) Upadhyay, S. K. *Chemical Kinetics and Reaction Dynamics* **2006**, DOI: 10.1007/978-1-4020-4547-9.
(34) Steinfeld, J. I.; Francisco, J. S.; Hase, W. L. *Chemical Kinetics and Dynamics*; Prentice Hall: 1989.
(35) Hayden, P.; Melville, H. J. *J. Polym. Sci.* **1960**, *43*, 201−214.
(36) Doi, M. *Chem. Phys.* **1975**, *9*, 455−466.
(37) Guzmán, J. D.; Pollard, R.; Schieber, J. D. *Macromolecules* **2005**, *38*, 188−195.
(38) Doi, M.; Edwards, S. F. *The Theory of Polymer Dynamics*; Oxford University Press: New York, 1986.

DOI: 10.1021/acs.nanolett.9b00163
Nano Lett. 2019, 19, 2032−2036